ELSEVIER

Journal of Non-Crystalline Solids 265 (2000) 41–50

JOURNAL OF NON-CRYSTALLINE SOLIDS

www.elsevier.com/locate/jnoncrysol

Structure of silica-based organic–inorganic hybrid xerogel

Bruno Boury [a], Robert J.P. Corriu [a,*], Pierre Delord [b], Valérie Le Strat [a]

[a] *Laboratoire de Chimie Moléculaire et Organization du Solide, UMR 5637, Université Montpellier II, Place E. Bataillon, 34095 Montpellier cedex 5, France*

[b] *Groupe de Dynamique des Phases Condensées, UMR 5581 Université Montpellier II, Place E. Bataillon, 34095 Montpellier cedex 5, France*

Received 12 July 1999; received in revised form 26 October 1999

Abstract

The short range order in hybrid xerogels obtained by hydrolysis of $(MeO)_3Si–C{\equiv}C–C_6H_4–C{\equiv}C–Si(OMe)_3$ was investigated by X-ray diffraction analysis. Results were correlated to spectroscopic data and porosity measurements. Aside from the signal related to the Si–O–Si units ($q = 1.60$ Å^{-1}), the signals at $q_1 = 0.55$ Å^{-1} and $q_2 = 1.12$ Å^{-1} were attributed to the presence of organic spacers and their organization within the material. These signals were found to be independent of the porosity of the material as measured by the BET method. Thus, changing the solvent or the concentration used at the polycondensation step leads apparently to a similar structure for the materials, representative of the same local order in the material although the porosity is very different. Copolycondensation with tetramethoxysilane (TMOS) results in a shift of the q_1 broad peak towards small angles and a decay of the q_2 signal when increasing TMOS ratio. An interpretation by a uniaxial swelling is proposed. Elimination of the organic group by chemical treatment and thermal treatment leads to silica xerogels. While no traces of the former organization were found in the case of chemical treatment, the presence of a signal at about 0.30 Å^{-1} indicates the possibility of a residual organization in the case of the thermal treatment.

1. Introduction

A special class of hybrid nanostructured materials can be prepared by sol–gel polycondensation of precursors of the general formula $(MeO)_3Si–R–Si(OMe)_3$ (Scheme 1) [1–7]. They raise interesting questions about their porosity and their structure. From a qualitative point of view, it was proposed that the porosity of this solid is kinetically controlled and also depends on the interactions between the solvent and the solid phase [8]. In addition, it was demonstrated that the nature of the bridging organic group is a key parameter that can influence the porosity: rigid aryl groups like the phenylene or polyphenylene group providing a generally porous solid [8–11], while flexible alkyl groups, like polymethylene groups, lead to non-porous solids [12–14].

Concerning the organization of these materials, the chemical transformation in the solid state of some of these xerogels suggests the possibility of a short-range order. For example, it is possible to induce the electrochemical and chemical polymerization of thiophene units in $(O)_{1.5}Si–(C_4H_4S)–Si(O)_{1.5}$ [15] or the thermal crosslinking reaction of acetylenic units in $(O)_{1.5}Si–C{\equiv}C–C{\equiv}C–Si(O)_{1.5}$ [16]. These chemical tools demonstrate that these rigid organic groups are spatially close enough to

* Corresponding author.
E-mail address: cmos@crit.univ-montp2.fr (R.J.P. Corriu).

0022-3093/00/$ - see front matter
PII: S0022-3093(99)00689-4

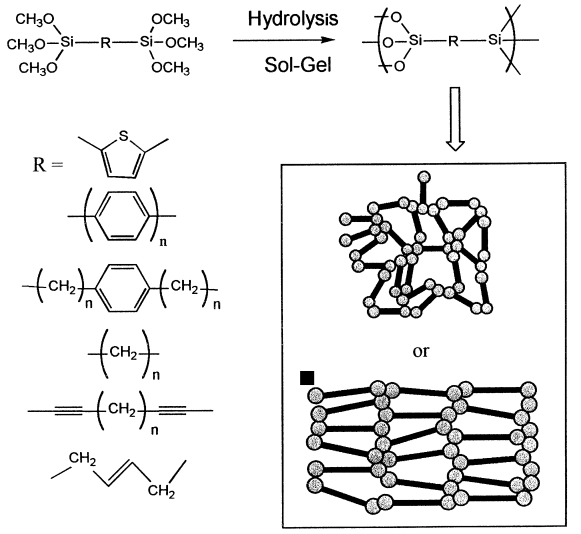

Scheme 1.

react with each other. However, the structure of these materials is not clearly understood at the present time. Initially, a two-dimensional structure covalently or hydrogen bonded was proposed and compared with molecular simulations [17].

SAXS and USAXS (Small and ultra small angle X-ray scattering) measurements have been performed on three types of hybrid xerogels: $O_{1.5}Si$–C≡C–C_6H_4–C≡C–$SiO_{1.5}$ [9], $O_{1.5}Si$–C≡C–$(CH_2)_n$–C≡C–$SiO_{1.5}$ ($n=4$ and 8) [13] and $O_{1.5}Si$–$(C_6H_4)_n$–$SiO_{1.5}$ ($n=1$, 2 and 3) [8]. For these materials, the covalent bonding between the organic and the inorganic parts implies a monophasic material. Since SAXS analysis is sensitive to the fluctuations of the electronic density in the medium, an analysis of the SAXS data for these materials encounters some difficulties because of several sources of contrast in the medium. First, the porosity leads to an important scattering at small angles due to the high contrast of the electronic densities between the void and the material. Secondly, fluctuations of electronic density also arise from the presence of two additional domains, each having its own electronic density: the organic moieties and the siloxane network. Moreover, power laws are observed but generally in too narrow intervals of q for very convincing interpretations. Nevertheless, a slope of $\geqslant -3$ was observed for $O_{1.5}Si$–$(C_6H_4)_n$–$SiO_{1.5}$ ($n=1$, 2 and 3). The Porod law q^{-4} is not observed, indicating the absence of a clear-cut electron density between two phases, generally representing a net surface in porous materials. For example, we have observed similar results with a power law of $q^{-2.3}$ for $O_{1.5}Si$–C≡C–$(CH_2)_4$–C≡C–$SiO_{1.5}$ and q^{-3} for $O_{1.5}Si$–C≡C–$(CH_2)_8$–C≡C–$SiO_{1.5}$ [13]. All these results suggest a surface with fractal geometry.

Some of these hybrid xerogels were also studied by X-ray diffraction analysis and found generally amorphous. However, X-ray diffraction analysis of some of these hybrid xerogels has revealed the presence of one or several unexpected signals in the 0.1 $\text{Å}^{-1} < q < 1.5$ Å^{-1} region along with the broad signal related to the Si–O units of the silica network $q = 1.6$ Å^{-1}: for $O_{1.5}Si$–$(C_6H_4)_3$–$SiO_{1.5}$ and possibly $O_{1.5}Si$–$(C_6H_4)_2$–$SiO_{1.5}$ [8], for $O_{1.5}Si$–C_6H_4–$SiO_{1.5}$ [10] and for the $O_{1.5}Si$–C≡C–C≡C–$SiO_{1.5}$ [16].

We focused our studies on xerogels prepared from a precursor with a rigid rod-like geometry, the 1,4-Bis[(trimethoxysilyl)ethynyl]benzene **1** (Scheme 2). We recently showed that chemical treatment of the corresponding xerogel, $O_{1.5}Si$–C≡C–C_6H_4–C≡C–$SiO_{1.5}$, leads to the formation of carbon-free silica with a narrow pore size distribution due to the Si–C_{sp} hydrolysis and the elimination of the HC≡C–C_6H_4–C≡CH group [9,18].

In this paper, we present the results of X-ray experiments performed in order to detect a possi-

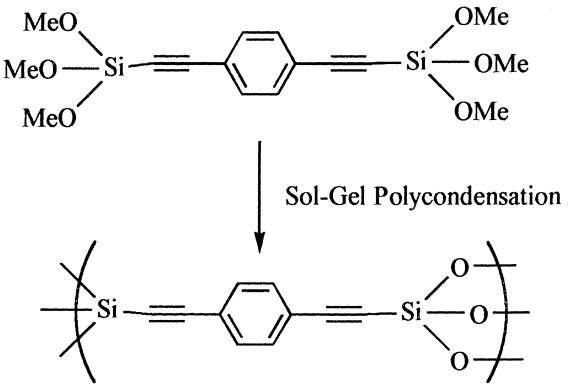

Scheme 2.

ble medium or short-range order in this material. To look more closely at its structure, we investigated the $0.1\ \text{Å}^{-1} < q < 2.5\ \text{Å}^{-1}$ domain since it corresponds to a short-range structural organization. This analysis was performed on a family of xerogels of general formula $O_{1.5}Si–C{\equiv}C–C_6H_4–C{\equiv}C–SiO_{1.5}$ and prepared by different experimental procedures (solvent, concentration, catalyst and using TMOS as co-reagent). Additionally we analyzed the carbon-free silica obtained by removal of the organic spacer by thermal or chemical treatment.

2. Experimental

Preparation of the 1-4-Bis[(trimethoxysilyl)ethynyl]benzene (**1**) and hybrid xerogels along with their analyses (NMR spectroscopy, BET, elemental analysis) before and after gelation were previously reported [9]. The hydrolysis and condensation of the linear rigid precursor are performed by sol–gel process in the absence of a catalyst (excepted when specified) as described in a previous reference [9]. A homogeneous mixture of precursor, solvent and deionized water (pH = 6) is prepared at room temperature and kept without stirring. After gelation, gels were allowed to stand for 8 days for aging at room temperature and then crushed, washed with ether and dried in vacuum at 120°C for 24 h.

The X-rays experiments were performed on several apparatus, either on a classical $\theta - 2\theta$ goniometer or an imaging plate two-dimensional detector with a rotating anode apparatus. The radiation is Cu Kα ($\lambda = 1.542$ Å) for both. The samples ground in an agate mortar, were put in a 1 mm diameter, 8 mm length glass Lindeman capillary or between two sticky capton plates. In this last case the samples were about 45 μm thick. It is noteworthy that capton gives a diffraction peak at 0.4 Å^{-1}. Also the glass capillary tube shows a peak for SiO_2 at about 1.7 Å^{-1}. In the case of the θ–2θ goniometer, the spectra were recorded between $0.21 < q < 2.79\ \text{Å}^{-1}$ ($q = 4\pi \sin\theta/\lambda$) The step was $7.10^{-3}\ \text{Å}^{-1}$, with an acquisition time on each step of 140 s. When the imaging plate apparatus was used, the acquisition time was 600–1200 s. The distance between source and detector was 150 mm and the diameter of the plate was 180 mm.

^{29}Si NMR solid state spectra were obtained using the CP MAS method, the contact time was 2000 μs, with 1389 scans, 10 s of recycle time and a spinning rate of 5 MHz. Surface area measurements were conducted on a porosimeter using high purity N_2 as adsorbate at 77 K and equilibrium analysis mode. Equilibration time was 5 s. A 35 points adsorption–desorption isotherm plot was obtained. The surface area was calculated using the BET equation [19,20]. The BJH equation applied to the isothermal desorption branch gave the pore diameter distribution by plotting $[dV/d\log(D)]$ vs pore diameter [21]. The evaluation of total microporous volume was done by the *t*-plot method.

3. Results

3.1. Preparation of the hybrid xerogel

General consideration. All the hybrid xerogels were prepared using the 1-4-Bis[(trimethoxysilyl)ethynyl]benzene **1** as precursor. The conditions used for the preparation of the materials were previously reported and are summarized in Scheme 3 and the related Table 1 [9,13].

Solvent effect. THF and methanol were used as respectively protic and aprotic polar solvent in order to compare their impact on the characteristics of the xerogel ($\mathbf{H}_1$ and $\mathbf{H}_2$).

Precursor's concentration effect. In order to determine the influence of the precursor's concentration on the gelation process, preparation of the xerogel was performed using three different concentrations of **1** in THF ($\mathbf{H}_1$, $\mathbf{H}_3$ and $\mathbf{H}_4$).

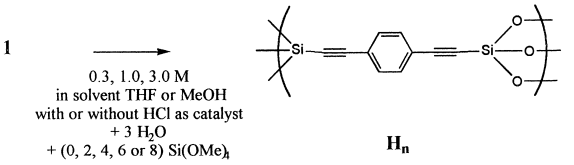

Scheme 3.

Table 1
Experimental parameters used for the preparation of $\mathbf{H}_{1-9}$

	Solvent	Concentration (mol l^{-1})	HCl catalyst (precursor/HCl molar ratio)	Co-reagent (precursor/TMOS molar ratio)	Specific surface area (m^2 g^{-1}) (±5%)
$\mathbf{H}_1$	THF	3			25
$\mathbf{H}_2$	CH_3OH	3			905
$\mathbf{H}_3$	THF	1			<10
$\mathbf{H}_4$	THF	0.3			<10
$\mathbf{H}_5$	THF	3		TMOS (1/2)	35
$\mathbf{H}_6$	THF	3		TMOS (1/4)	15
$\mathbf{H}_7$	THF	3		TMOS (1/6)	<10
$\mathbf{H}_8$	THF	3		TMOS (1/8)	<10
$\mathbf{H}_9$	THF	3	2×10^{-2}		25

Co-gelation effect. We also prepared hybrid gels upon co-hydrolysis and condensation of the precursor **1** in the presence of variable amounts of $Si(OMe)_4$ ($\mathbf{H}_1$, $\mathbf{H}_5$, $\mathbf{H}_6$, $\mathbf{H}_7$ and $\mathbf{H}_8$).

Catalyst effect. All the above experiments were performed in the absence of any catalyst due to the high reactivity of this precursor. However, we investigate the effect of a catalyst like HCl that we used at a 2% molar concentration ($\mathbf{H}_1$ and $\mathbf{H}_9$). Other catalysts like nucleophile (F^-) or base (NH_3) can be used [22]; however they must be avoided in the present case since they can promote the hydrolysis of the Si–C*sp* bond [9,13,16].

Chemical and thermal treatment effect. In another experiment, hybrid xerogels prepared in THF at a 3 M concentration ($\mathbf{H}_1$) were treated in order to remove the organic spacer. This was performed by two different routes: one via thermal oxidation leading to $\mathbf{T}_1$ and the other one by a mild chemical treatment using NH_4F as catalyst (2%) leading to $\mathbf{C}_1$ (Scheme 4) [9]. These treatments are efficient for removing all the organic spacers from the material and a silica free of carbon is recovered in both cases.

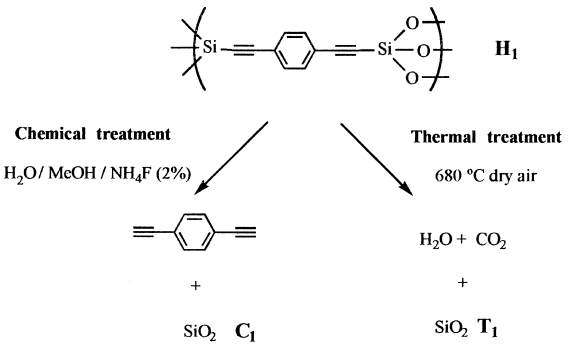

Scheme 4.

3.2. Characterization of the precursors (**1**) and the hybrid materials ($\boldsymbol{H}_{1-9}$)

Some of the spectroscopy analyses and surface area measurements were already reported for these materials [9]. Hence, data are mentioned here in order to complete the X-ray results performed in the range $0.1\ \text{Å}^{-1} < q < 2.5\ \text{Å}^{-1}$.

Precursor **1**. X-ray analysis of the precursor **1**, 1,4-Bis[(trimethoxysilyl)ethynyl]benzene, was performed with a Lindeman tube filled with **1** in the liquid state. One broad signal with large wings centered at $q = 1.17\ \text{Å}^{-1}$ is observed (Fig. 1). In our experiment, the precursor was a crystalline solid at room temperature (m.p.: 35–36°C) that exhibits the X-ray powder diffraction presented in Fig. 1.

Solvent effect. Gelation of **1** at a concentration of 3.0 mol l^{-1} in methanol or THF occurs within less than 1 min. From a structural point of view, X-ray analysis of the xerogel $\mathbf{H}_1$ (solvent THF) and $\mathbf{H}_2$ (solvent methanol) gives the same type of results: three broad signals are observed respectively centered at $0.55\ \text{Å}^{-1}$, $1.12\ \text{Å}^{-1}$ and $1.60\ \text{Å}^{-1}$ (Fig. 2). The spectroscopic data are the same for these xerogels; ^{29}Si CP MAS NMR analysis indicates the same set of signals at −79 ppm [T^1

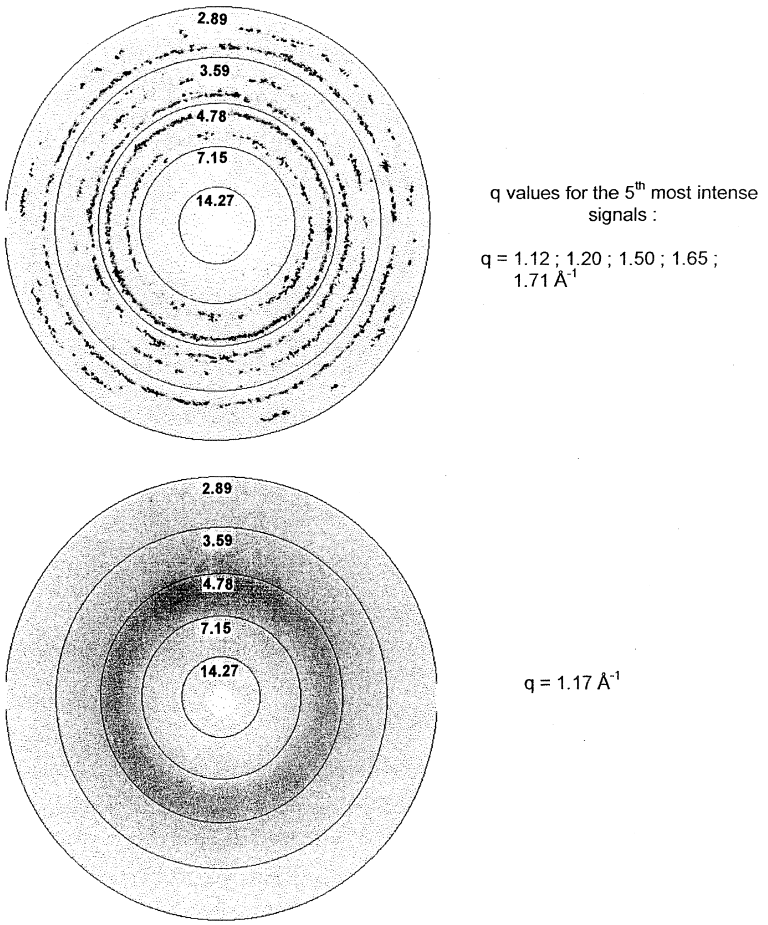

Fig. 1. X-ray analysis of the precursor in the solid state and the liquid.

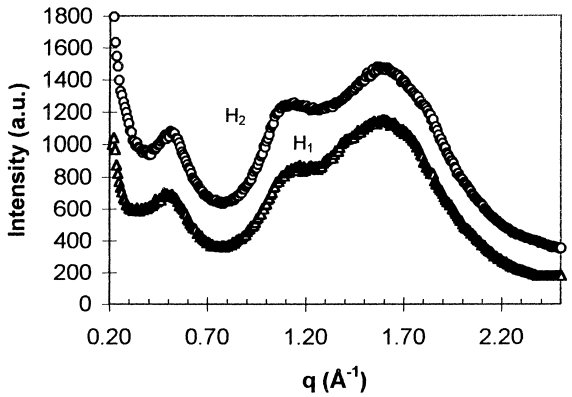

Fig. 2. X-ray powder diffraction of $\mathbf{H}_1$ and $\mathbf{H}_2$.

$CSi(OH)_2(OSi)]$, −87 ppm [T^2 $CSi(OH)(OSi)_2$] and at −95 ppm [T^3 $CSi(OSi)_3$], characteristic of a silicon atom attached to three oxygen and one *sp* carbon atoms. [1] If we now look to the porosity of these materials, it is noteworthy that they are highly different since specific surface areas are respectively 25 m^2 g^{-1} for $\mathbf{H}_1$ prepared in THF and

[1] To evaluate the local environment of the silicon atom in these xerogel, the CP MAS is a convenient sequence for solid state analysis. However, since the intensity of the signal is closely dependent on both the distance to and the number of hydrogen in the environment of the silicon atoms, the peak intensity does not accurately represent the population in the sample. Results are essentially qualitative.

905 m^2 g^{-1} for $\mathbf{H}_2$ prepared in methanol. The increasing intensity at very small q observed for $\mathbf{H}_2$ is due to its high specific surface area and porosity. These results show that the X-ray signals are totally independent of the porosity of the material since non-porous $\mathbf{H}_1$ and porous material $\mathbf{H}_2$ give exactly the same diffractogram. The effect of the porosity in the case of $\mathbf{H}_2$ is located at small angle q vectors. By the way, it can be assumed that the solvent used for the preparation of the xerogels is not the main parameter that influences the local structure and the relative organization of the organic group.

Concentration effect. For xerogels $\mathbf{H}_{1,3\text{-}4}$ prepared with different concentrations of precursor in THF, the X-ray analysis gives the same type of data: three broad signals are observed at 0.55 $Å^{-1}$, 1.12 $Å^{-1}$ and 1.60 $Å^{-1}$ (Fig. 3). These xerogels are all non-porous materials (<10 m^2 g^{-1}) and their spectroscopic data are similar to those of $\mathbf{H}_1$. Despite the qualitative aspect of the ^{29}Si NMR CP MAS analysis, comparison between these xerogels can be attempted due to the similarity of the materials. In both the cases we found the same relative intensity for the T^1, T^2 and T^3 signals, indicating the same level of polycondensation, despite very different gelation times: respectively 60×10^5, 420×10^5 and 6×10^5 s for $\mathbf{H}_1$, $\mathbf{H}_3$ and $\mathbf{H}_4$.

Co-gelation effect. The co-polycondensation of **1** with increasing proportion of TMOS (1 : 2, 1 : 4, 1 : 6, 1 : 8), in the absence of any catalyst, leads to hybrid xerogels with decreasing proportion of the organic part linked to the silica network. It is noteworthy to mention that gelation time increases with increasing proportion of TMOS. For example the gelation time is 1.0 min for pure **1**, 11×10^3 min for a (1 : 8) **1**/TMOS ratio and 18×10^3 for pure TMOS in the same experimental conditions. The specific surface area of the hybrid xerogels $\mathbf{H}_{5\text{–}8}$ decreases when the percentage of TMOS is increased going from 35 m^2 g^{-1} to <10 m^2 g^{-1}. The ^{29}Si CP MAS NMR spectra present the signals associated with T^n substructures coming from **1** and the Q^n substructures coming from the TMOS. The major signals correspond to T^2 [$CSi(OH)(OSi)_2$ or $CSi(OMe)(OSi)_2$] substructure at −87 ppm and Q^3 [$Si(OH)(OSi)_3$ or $Si(OMe)(SiO)_3$] substructure at −101 ppm. The X-ray curves of these xerogels are presented in Fig. 4 which clearly shows an evolution of the signal with the variation of the (**1**:TMOS) ratio in the starting mixture. The signal at 0.55 $Å^{-1}$ for $\mathbf{H}_1$ shifts toward small angles progressively with increasing proportion of TMOS, finally a signal at 0.40 $Å^{-1}$ for **1**:TMOS = 8 is observed ($\mathbf{H}_8$). We also found that signal at 1.12 $Å^{-1}$ decreases in intensity with increasing proportions of TMOS to finally disappear for **1**:TMOS = 8 ($\mathbf{H}_8$).

Catalysis effect. $\mathbf{H}_9$ is the xerogel prepared in the presence of HCl as catalyst. It presents the same X-ray diffractogram as $\mathbf{H}_1$ prepared in the same conditions but in the absence of any catalyst: broad signals at 0.55 $Å^{-1}$, 1.12 $Å^{-1}$ and 1.60 $Å^{-1}$. The gelation times are the same in both cases and the presence of the catalyst does not shorten it. On

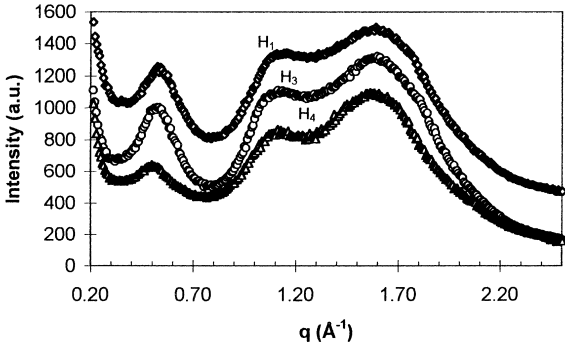

Fig. 3. X-ray powder diffraction of $\mathbf{H}_1$, $\mathbf{H}_3$ and $\mathbf{H}_4$.

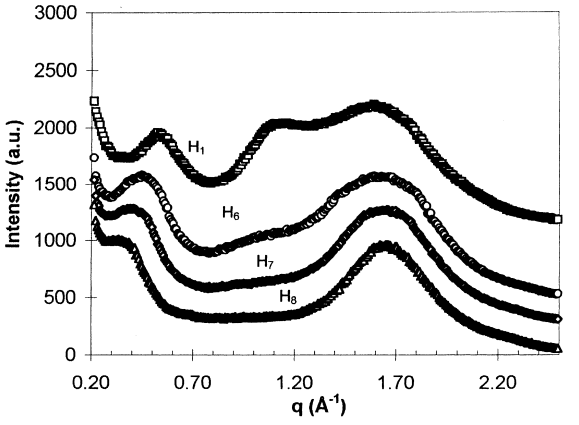

Fig. 4. X-ray powder diffraction of xerogel of $\mathbf{H}_1$, $\mathbf{H}_6$ and $\mathbf{H}_7$ and $\mathbf{H}_8$.

the other hand, $\mathbf{H}_1$ and $\mathbf{H}_9$ are both non-porous materials with specific surface area around 25 m^2 g^{-1}. For $\mathbf{H}_9$, ^{29}Si CP MAS NMR analysis indicates the same set of signals than for $\mathbf{H}_1$: −79 ppm, −87 ppm and −95 ppm. As done previously, a comparison of these results for $\mathbf{H}_1$ and $\mathbf{H}_9$ can be attempted due to the similarity of the materials. In both cases we found the same relative intensity for the T^1, T^2 and T^3 signals. Finally it appears that neither the porosity nor the organization is modified by the presence of HCl.

Chemical treatment and thermal treatment. The carbon-free silica $\mathbf{C}_1$ obtained by chemical treatment of $\mathbf{H}_1$ is a mesoporous material with a specific surface area of 655 m^2 g^{-1} and a narrow pore size distribution centered at 50 Å. SAXS measurement shows a q^{-4} slope of the spectrum at small q values, in the so-called Porod domain that indicates a clear cut change in density between the solid silica phase and the void following Porod's law [9]. X-ray diffractogram is similar to silica obtained from TMOS, only a broad signal at 1.55 $Å^{-1}$ is observed. An increasing intensity related to the high porosity of this material is observed for the lowest q values (Fig. 5). These results undoubtedly confirm the previous data showing a total elimination of the organic spacer.

Total elimination of the organic spacer was achieved as well by thermal treatment as evidenced by elemental analysis. However, porosity data of $\mathbf{T}_1$ are completely different from those of $\mathbf{C}_1$. Both specific surface area value (430 m^2 g^{-1}) and the pore size distribution (centered around $\varnothing < 15$ Å) obtained from the desorption plot indicate that the material is mainly a microporous one. Characterization by SAXS measurements indicates a power law in q^{-4}, between 10^{-3} $Å^{-1}$ and 1.5×10^{-2} $Å^{-1}$ and in $q^{-3.3}$ between $0.06 < q < 1.50$ $Å^{-1}$. In that case, the X-ray diffractogram presents two signals, a broad one located at 1.56 $Å^{-1}$ like for usual silica and another signal at low q values, 0.30 $Å^{-1}$ (Fig. 5). This signal is shifted to lower q values, compared to the initial signal observed for the hybrid starting material. Since this material is free of any spacer residue, the presence of this signal can be seen as a remainder of structural organization. From this point of view, it might be seen as evidence for a phenomenon of molecular imprint, however with a very rough definition.

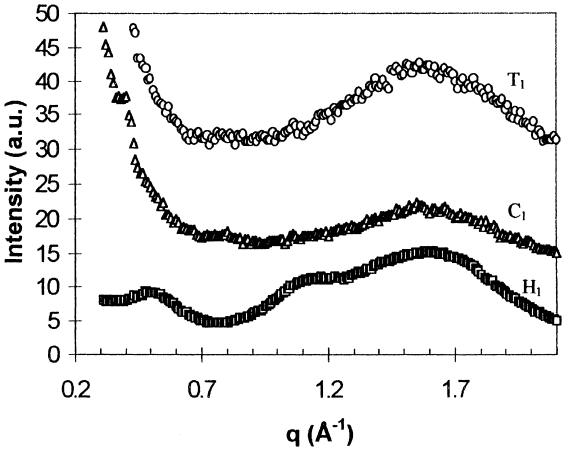

Fig. 5. X-ray powder diffraction of $\mathbf{H}_1$, $\mathbf{C}_1$ and $\mathbf{T}_1$.

4. Discussion

Hybrid xerogels are generally considered to be amorphous materials. In the case of another arylene rigid precursor, the authors proposed the formation of aggregates based on calculations and NMR data [17]. The present results point out the presence of signals on diffractogram curves related to the presence of the organic spacer. They disappear with the elimination of the organic spacer by chemical treatment and they are modified or shifted by the presence of a co-reagent like TMOS. As a consequence, we consider the possibility to relate the presence of such signals to the organization of the material and more precisely to the short-range organization of the organic groups.

The distance associated with the first peak at $q_1 = 0.55$ $Å^{-1}$ by a Bragg law corresponds to $d = 2\pi/q = 11.4$ Å, close to the Si...Si distance in the organic spacer as determined by molecular simulation (d Si_1...Si_2: 11.45 Å). Certainly, this first peak is too large to be interpreted in terms of crystalline periodicity on a long range. However, a short-range order in the hybrid xerogel can be considered, this organization being favored by the presence of the rigid organic unit. For the second

peak at $q_2 = 1.12$ Å^{-1} two possibilities can be suggested. First, the value for this signal could be attributed to a possible stacking of the spacers. However, one may observe that $q_2 = 2q_1$ and, in addition, the possibility of a third peak at $q_3 = 3q_1$ masked by the silica bump has to be considered. In this case, another interpretation may be proposed: we could be seeing a modulation of the intensity by an interference function corresponding to a disorder of the second kind, as described in the literature [23–25]. In this assumption, the broad peaks at q_1, q_2 and q_3 are related to a mean spacing $d = 2\pi/q1 = 11.4$ Å between stacked structural units, the damping of the oscillations arising from the loss of spatial correlation in the units' position: the stronger is the damping, the smaller is the correlation length in the material. In the present case, the structural units may comprise some spacers stacked and bounded together by Si–O–Si chain skeletons as depicted in a simplified way on Scheme 5. The stacking law of the rigid spacers and the repetition law of the structural unit are not known at the moment.

Such rigid structural units are very different in two spatial orthogonal directions. The direction along the rigid spacers takes into account the repetition law of the spatial units. The perpendicular direction takes into account the contiguous arrangement of spacers. Unfortunately, at the scale of the dimension of the X-ray beam, the samples are isotropic and since experiments are made on powders, the results are spherically averaged. Only X-ray diffraction on oriented samples could allow the removal of this ambiguity. Also, an effort is actually made in our laboratories, to control the kinetics of gel formation and to obtain optically anisotrope xerogels.

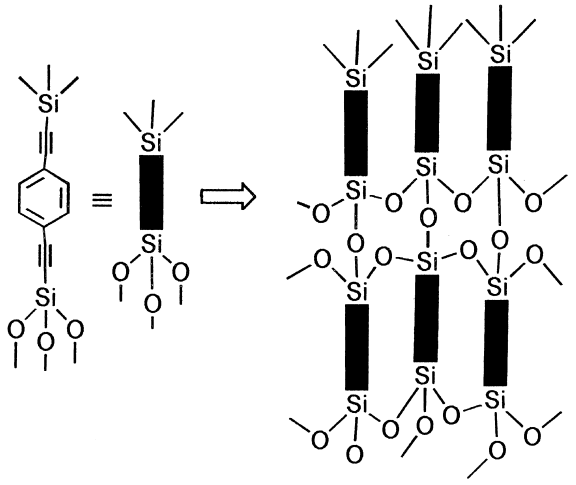

Scheme 5.

A quantitative interpretation being not possible at the present time, a qualitative discussion can be proposed with a one-dimensional short-range order hypothesis. It first appears that the structural organization of the material is apparently independent of experimental parameter like the nature of the solvent, the concentration or the presence of a catalyst like HCl and all parameters that can modify the kinetic of the polycondensation. In fact, we found in some case a modification of the porosity (solvent effect) but no modification of the structure, as revealed by the diffractograms.

The most convincing results, strengthening the previous hypothesis, are provided by the copolymerization with TMOS. We plot the $q_{1,n}$ value vs the volume fraction of SiO_2 introduced via TMOS, n being the number of added SiO_2 molecules by molecule of precursor; we see that the first peak is shifted towards small q values and that $q_{1,n}$ evolves linearly with the volume fraction of silica added by copolymerization, φ_{SiO_2}. This is a strong indication of a uniaxial swelling. The experimental swelling law is $q_{1,n} = q_{1,0}(1 - 0.48\varphi_{SiO_2})$. This result has to be compared with a pure swelling where the added silica is involved in the swelling. The pure swelling law is $q_{1,n} = q_{1,0}(1 - \varphi_{SiO_2})$. It is easy to see that the experimental swelling is smaller than a pure swelling. These results support the hypothesis that the TMOS does not polycondense as a separate material but is inserted in the material between precursors units. Moreover, the gradual vanishing of the second peak $q_{2,n}$ with increasing TMOS ratio, shows a loss of correlation between the layers. The discrepancy between the experimental and the pure swelling laws results from the fact that all the silica added by the polycondensation of TMOS does not induce a 'pure' swelling. This ideal situation is represented in Scheme 6(a) and would correspond to the theoretical curve in Fig. 6. On the contrary, the situation presented in

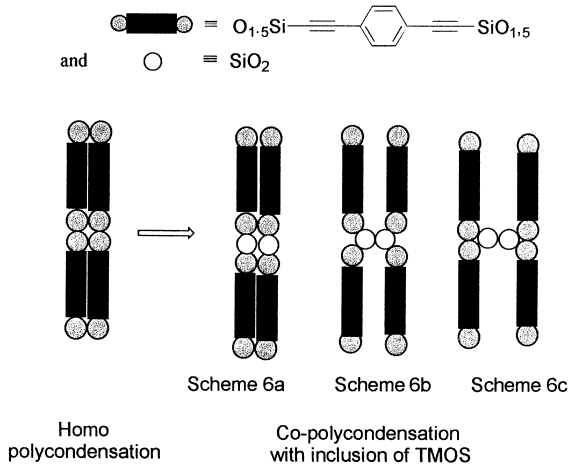

Scheme 6.

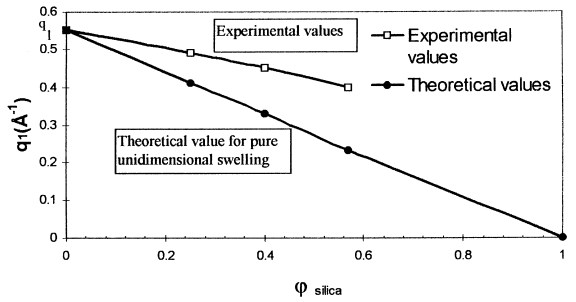

Fig. 6. Variations of q_1 values with φ_{silica}.

Scheme 6(c) should correspond to inclusion of silica units between organic units without swelling of the lamellar structure. Experimental results support an intermediate situation where silica units produce both a swelling of a locally lamellar structure and a spacing between contiguous molecules of the precursor represented in Scheme 6(b). One may qualitatively estimate the shared ratio at about 50%.

These results agree with the chemical reactivity of respectively the 1,4-Bis[(trimethoxysilyl)ethynyl]benzene **1** and the TMOS. The highest reactivity of the hybrid precursor compared to TMOS is evidenced by its short gelation time (±1.0 min) compared to TMOS (18×10^3 min). It suggests that the hydrolysis of **1** generates reactive species able to condense either with themselves by homopolycondensation or with TMOS by co-polycondensation, the homo-polycondensation being favored at a low proportion of TMOS. Inclusion of TMOS is efficient only at high proportion of TMOS. According to this process, a random polycondensation promoted via hydrolyzed precursor **1** leads to a homogeneous distribution of the precursors and silica. Therefore, increasing the proportion of TMOS favors the incorporation of silica units and limits the possibility of polycondensation of **1** with itself.

From a general point of view, we did not observe strong differences in the local structure generated with a set of different chemical conditions. At the same time, the porosity of the material appeared closely related to the nature of the solvent that was used, THF leading to a non-porous material while porous materials are obtained with methanol. These results support the idea that the porosity and the local structure of the materials arise from two different phenomena. We can assume that the local structure from X-ray data results from the association of the monomers between each other in the clusters, the aggregates and the colloids, while the porosity is certainly more related to the interaction between these objects (particles, aggregates and colloids) and the solvent. Such an idea was already proposed in the case of arylene-bridged polysilsequioxanes [8] and is currently under investigation in our laboratories.

Finally, results obtained with $\mathbf{C}_1$ indicate that the chemical treatment of $\mathbf{H}_1$ occurs with a complete loss of the organization present in the hybrid xerogel which is related to the organic spacer. Such reorganization is facilitated by the low degree of polycondensation of the initial $\mathbf{H}_1$ and also by the activation of the Si–O bond by F^- anion that can catalyze the hydrolysis, redistribution and polycondenzation of the silica network. These combined processes can lead to the formation of aggregates and colloids that are free to recombine to form the residual silica as previously reported [9,13,18].

5. Conclusion

The reported results point out the presence of a short-range order in these hybrid xerogels

prepared by the sol–gel process using a precursor with a rigid rod-like geometry. In the present case it has a one-dimensional character, perhaps locally lamellar, which suggests a tendency of the hybrid molecules to an ordering aggregation. Under such conditions it is not surprising that a hybrid is not the best choice for molecular imprinting [18]. The organization is apparently not modified by parameters like the nature of the solvent, the concentration of precursor or the use of a catalyst. While they can modify the texture of the solid, these kinetic parameters do not promote a variation of the short-range order. The nature of the precursor is certainly a key parameter of the organization of the organic moieties. In contrast, evolution of this structure can be promoted by using a co-reagent like TMOS that can be seen as a tool for the investigation of the structure.

References

[1] G. Cerveau, R.J.P. Corriu, Coord. Chem. Rev. 180 (1998) 1051.
[2] R.J.P. Corriu, C.R. Acad. Sci. Paris 1 (1998) 83.
[3] R.J.P. Corriu, D. Leclercq, Angew. Chem., Int. Ed. Engl. 35 (1996) 4001.
[4] R.J.P. Corriu, Polyhedron 17 (1998) 925.
[5] R.H. Baney, M. Itoh, A. Sakakibara, T. Suzuki, Chem. Rev. 95 (1995) 1410.
[6] C.C. Sanchez, F. Ribot, New J. Chem. (1994) 989.
[7] D.A. Loy, K.J. Shea, Chem. Rev. 95 (1995) 1431.
[8] D.W. Schaefer, G.B. Beaucage, D.A. Loy, T.A. Ulibarri, E. Black, K.J. Shea, R.J. Buss, in: B.K. Coltrain, C. Sanchez, D.W. Schaefer, G.L. Wilkes (Eds.), Better Ceramics Through Chemistry VII; Organic/Inorganic Materials, Materials Research Society, Pittsburgh, PA, 1996, p. 301.
[9] P. Chevalier, R.J.P. Corriu, P. Delord, J.J.E. Moreau, W.C.H. Man, New J. Chem. (1998) 423.
[10] R.J.P. Corriu, J.J.E. Moreau, P. Thépot, M. Wong Chi Man, Chem. Mater. 4 (1992) 1217.
[11] K.J. Shea, D.A. Loy, Webster, J. Am. Chem. Soc. 114 (1992) 6700.
[12] W.H. Oviatt, K.J. Shea, H.J. Small, Chem. Mater. 5 (1993) 943.
[13] B. Boury, P. Chevalier, R.J.P. Corriu, P. Delord, J.J.E. Moreau, M. Man Wong Chi, Chem. Mater. 11 (1999) 281.
[14] G. Cerveau, R.J.P. Corriu, C. Lepeytre, H. Mutin, J. Mater. Chem. 8 (1998) 2707.
[15] R.J.P. Corriu, J.J.E. Moreau, P. Thépot, M. Wong Chi Man, C. Chorro, J.P. Lèreporte, J.L. Sauvajol, Chem. Mater. 6 (1994) 15.
[16] R.J.P. Corriu, J.J.E. Moreau, P. Thepot, M. Wong Chi Man, Chem. Mater. 8 (1996) 100.
[17] J.L. Faulon, D.A. Loy, G.A. Carlson, K.J. Shea, Comput. Mater. Sci. 3 (1995) 334.
[18] B. Boury, R.J.P. Corriu, P. Delord, V. Le Strat, New J. Chem. 23 (1999) 531.
[19] S. Lowell, J.E. Shields, Powder Surface Area and Porosity, Chapman and Hall, London, 1984.
[20] S.J. Gregg, K.S.W. Sing, Adsorption Surface Area and Porosity, Academic Press, London, 1982.
[21] E.P. Barrett, L. Joyner, P.P. Halenda, J. Am. Chem. Soc. 73 (1951) 373.
[22] C.J. Brinker, R. Sehgal, S.L. Hietala, R. Deshpande, D.M. Smith, D. Loy, C.S. Ashley, J. Membr. Sci. 94 (1994) 85.
[23] A. Guinier, Théorie et Technique de la Radiocrystallographie, Dunod, Paris, 1955.
[24] L.D. Landau, Zh. Eksperim. Teor. Fiz. 7 (1937) 1227.
[25] B.K. Vainshtein, Diffraction of X-rays by Chain Molecules, Elsevier, New York, 1966.